DOI: 10.1002/ejoc.200600107

# Anionic and Photochemical Behaviour of the Medium-Sized Terpenoid Ketone 8-Dehydro-12-*O*-methyl-deacylhallerin

**Gianluca Croce,[a] Marco Milanesio,*[a] Davide Viterbo,[a] Marco Clericuzio,[b] Piero Ugliengo,[c] and Giovanni Appendino[d]**

*Dedicated to the memory of Anna Ramella Pralungo[‡]*

**Keywords:** Terpenoids / Isomerization / Photochemistry / Molecular modelling / X-ray diffraction

Treatment of the germacrane ketone 8-dehydro-12-*O*-methyl-deacylhallerin (**2**) with bases under conditions of thermodynamic enolization resulted in complete epimerization at the adjacent carbon atom C-7, with formation of **3**. The conformational features of the epimeric ketones **2** and **3** were investigated by X-ray crystal structure analysis, NMR spectroscopy, molecular mechanics and dynamics simulations and ab initio calculations. While **2** showed temperature-insensitive sharp $^1$H NMR signals, its epimer **3** showed only broad lines. These spectral features suggest that **2** is monorotameric, while **3** is a mixture of different conformers, as was verified by molecular mechanics and dynamics calculations. Upon UV irradiation, **2** underwent isomerization at the C1–C10 double bond, while **3** was unreactive.


## Introduction

Germacranes are a group of sesquiterpenoids characterized by cyclodecane rings. Over 800 different compounds of this type have been isolated from plants, liverworts, insects and marine organisms, testifying to the relevance of this skeleton in natural products.[1] The biogenesis of germacranes is in principle simple, involving only the head-to-tail cyclization of farnesyl pyrophosphate. Nevertheless, germacrane derivatives are the precursors of a multitude of polycyclic terpenoid skeletons, formed through different rearrangements of their medium-sized rings.[2] These rearrangements are mediated by the formation of cationic intermediates, readily generated by treatment of germacrane olefins with acidic and/or electrophilic reagents.[3,4] Much less is known about the anionic rearrangements of this type of compounds,[5] as well as about their photochemical behaviour.[6,7] To complement previous studies on the cationic rearrangements of medium-sized terpenoids,[8,9–11] we have now investigated the behaviour of the enone **2** toward bases and light, supporting the experimental results with X-ray crystal structure data and theoretical molecular dynamics (MD) and quantum chemical calculations.

## Results and Discussion

The presence of a ketone carbonyl group was viewed as critical for induction of anionic and photochemical behaviour. Ketone **2** emerged as a suitable substrate because of its availability in multigram amounts by modification of the natural product hallerin (**1**)[8,10] and the presence of the reactive 1,4-diene system.

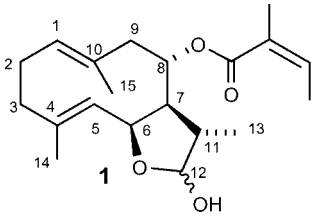


**1**

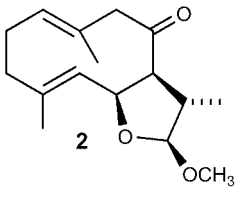


**2**

Enolization of **2** with LDA at –80 °C and subsequent protonation resulted in the recovery of the starting material,

[a] Dipartimento di Scienze e Tecnologie Avanzate, Università del Piemonte Orientale, "A. Avogadro",
Via Bellini 25/G, 15100 Alessandria, Italy
[b] Dipartimento di Scienze Ambientali e della Vita, Università del Piemonte Orientale "A. Avogadro",
Via Bellini 25/G, 15100 Alessandria, Italy
[c] Dipartimento di Chimica IFM and NIS – Nanostructured Interfaces and Surfaces – Centre of Excellence, Università di Torino,
Via P. Giuria 7, 10125 Torino, Italy
[d] Dipartimento. di Scienze Chimiche Alimentari Farmaceutiche e Farmacologiche, Università del Piemonte Orientale "A. Avogadro",
Via Bovio 6, 28100 Novara, Italy
[‡] *And it seems to me you lived your life*
*Like a candle in the wind*
("Candle in the wind", Elton John)
We dedicate this paper to the memory of Anna, whose recent death at the tragically early age of 33 came as a profound shock to her friends and colleagues. Anna was a lively and engaging young woman, dynamic, generous and life-loving. She was a committed, hard-working student, when she undertook the research described in this paper, which constitutes the substance of her master's thesis.

   

presumably as the product of enolization at the less substituted C-9 carbon atom and formation of a dienolate that was reprotonated without any rearrangement (Scheme 1). Conversely, treatment with sodium methoxide at room temp., afforded the C-7-epimeric derivative **3**, as the result of enolization at the more substituted carbon atom (C-7)[12] (Scheme 1). This suggests that the 7β-H configuration of **3** is preferred over that of **2**, as was backed up by ab initio calculations of the ground-state energies of the two stereoisomers (vide infra).

Remarkably, a C-8 carbonyl group is present in the very few 7β-H germacrane derivatives reported so far (8-oxocostunolide[13] and kurdione[14]), suggesting that they might be isolation artefacts.

Both **2** and **3** gave crystals suitable for X-ray diffraction analysis, and their X-ray molecular structures are shown in Figures 1 and 2, together with their labelling scheme.

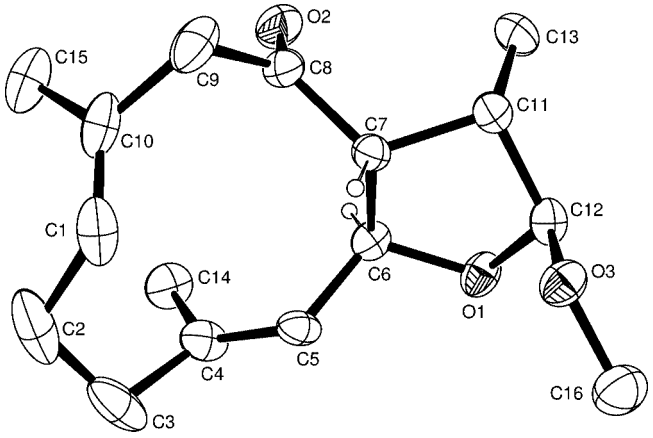


Figure 1. ORTEP plot of the crystal structure of epimer **2** with the atom labelling scheme and anisotropic thermal ellipsoids drawn at the 20% probability level.

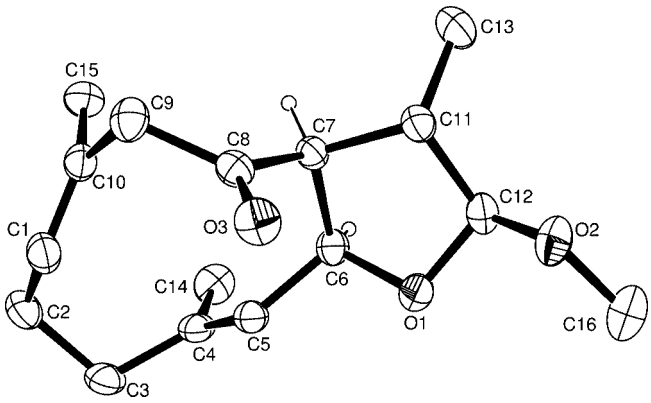


Figure 2. ORTEP plot of the crystal structure of epimer **3** with the atom labelling scheme and anisotropic thermal ellipsoids drawn at the 20% probability level.

In both compounds the two allylic methyl groups C14 and C15 are *syn* on the α-face of the diterpene system. Bond lengths and angles do not have abnormal values, but some angles show rather large differences between **2** and **3**: the 6° difference in the C8–C7–C11 bond angle may thus be a consequence of the different arrangement around C7, while the even larger difference (6.9°) in the C8–C9–C10 angle is probably due to the opposite orientation (on the β-face in **2** and on the α-face in **3**) of the ketone oxygen atom O3 with respect to the mean plane through the 10-membered ring. Table 1 lists the values of the torsion angles of the 10-membered rings of **2** and **3** and compares them with those of methylhallerin, in which C-8 is tetrahedral.[10] The conformation in **2** is quite similar to that of methylhallerin. As would be expected, the largest differences relate to the torsion angles involving C7. The fairly large variability of the geometrical parameters indicates that these compounds are endowed with a certain degree of flexibility, as is supported by the size of the thermal ellipsoids in Figures 1 and

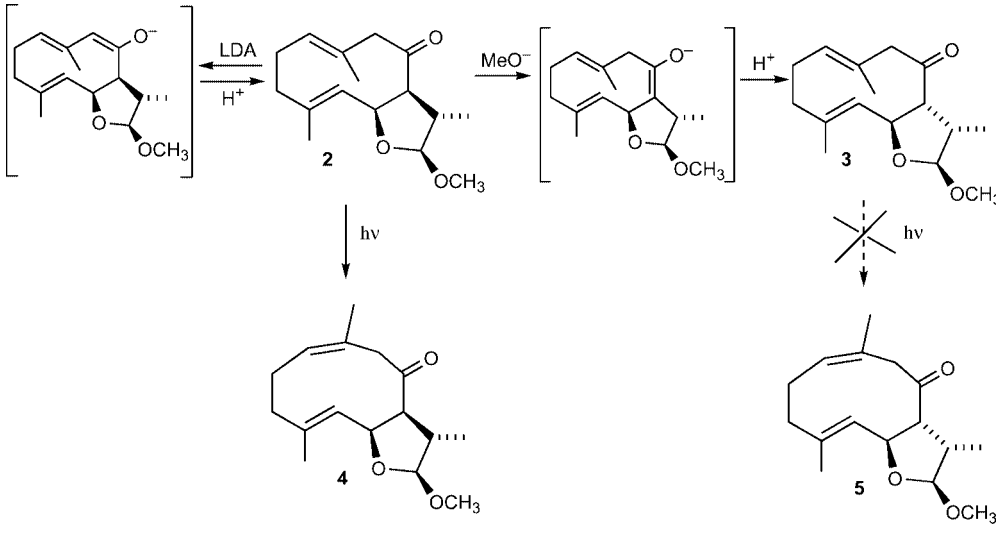


Scheme 1.

  

2. In Figure 1 we may note that all three oxygen atoms in **2** are directed towards the β-face of the cyclic core, with relatively short O···O nonbonded distances, while in **3** the oxygen atoms point in opposite directions and are rather distant (Table 2). This might be one of the factors contributing to the greater stability of **3** with respect to **2**.

Table 1. Comparison of the torsion angles of the 10-membered rings in **2**, **3** and in methylhallerin.[10]

| Torsion angle [°] | **2** | **3** | Methylhallerin |
|---|---|---|---|
| C9–C10–C1–C2 | –161.2 | –162.1 | –162.4 |
| C10–C1–C2–C3 | 99.0 | 110.2 | 92.8 |
| C1–C2–C3–C4 | –54.3 | –41.0 | –56.1 |
| C2–C3–C4–C5 | 87.5 | 97.0 | 84.9 |
| C3–C4–C5–C6 | –162.9 | –153.1 | –163.4 |
| C2–C3–C4–C14 | –84.6 | –73.7 | –88.0 |
| C4–C5–C6–C7 | 104.3 | 100.5 | 114.9 |
| C5–C6–C7–C8 | 30.0 | –88.4 | 25.7 |
| C6–C7–C8–C9 | –111.4 | 122.6 | –97.7 |
| C7–C8–C9–C10 | 62.4 | –92.0 | 55.8 |
| C8–C9–C10–C1 | 72.5 | 87.8 | 81.7 |
| C8–C9–C10–C15 | –104.3 | –85.6 | –95.1 |

Table 2. Comparison of the O···O nonbonded distances in the crystal structures of **2** and **3**.

| Distance [Å] | **2** | **3** |
|---|---|---|
| O1···O2 | 2.29 | 2.31 |
| O1···O3 | 3.23 | 4.08 |
| O2···O3 | 3.89 | 5.17 |

UV irradiation of **2** afforded a complete (*E*) → (*Z*) isomerization of the C1–C10 double bond, with formation of **4**. Comparison of the NMR spectra of **2** and **4** shows large differences in the chemical shift of the allylic methyl group C14: in the (*Z*) isomer the carbon atom resonates at lower fields ($\delta$ = 25.66 ppm) than in the (*E*) isomer ($\delta$ = 16.90 ppm). Since methylhallerin[10] was stable upon UV irradiation, the C=O group must be involved in the reaction. Apart from antenna effects, two mechanisms may be proposed for the isomerization (Scheme 2): a Norrish I fragmentation or a di-π-methane rearrangement. Remarkably, no isomerization to **5** took place (Scheme 1) when **3** was irradiated with UV light.

Compounds **2** and **3** show very different $^1$H NMR features. While the signals of **2** are sharp and unaffected by temperature changes, those of **3** show temperature-dependent broadening, suggesting that **2** is monorotameric in solution, while **3** has a greater conformational mobility and is a mixture of rotamers.

In order to obtain estimates of the relative stabilities of the four isomers **2**, **3**, **4** and **5**, we performed some DFT calculations at the B3LYP/6-31G(d,p) level, and their results are given in Table 3. For isomers **2** and **3** the conformations found in the X-ray structures were indicated as the most stable ones by conformational searching (vide infra) and were used for the quantum chemical calculations. We then also employed the most stable conformers found by a molecular mechanics search for the ab initio calculations on isomers **4** and **5**, for which no crystal structures were available. The reported values of the energy differences clearly indicate that the 7α epimer **3** is more stable than the 7β epimer **2**, thus implying that the complete epimerization reaction by treatment of the natural 7β epimer **2** with strong bases gives a significantly more stable compound. The photoisomerization reactions – **2** → **4** and **3** → **5** – do not produce appreciable energy changes and kinetic factors must play a role: the less stable epimer **2**, when irradiated with UV light, undergoes the isomerization reaction to **4**, while the more stable epimer **3** would require too high an activation energy for the photoisomerization to occur.

We next carried out a systematic conformational search on the two epimers **2** and **3** in an attempt to explain the differences in their NMR spectra. The search was performed with use of the SYBIL force-field[15] and the Osawa method,[16] as implemented in the molecular mechanics module of Spartan,[17] and the most stable conformers (rela-

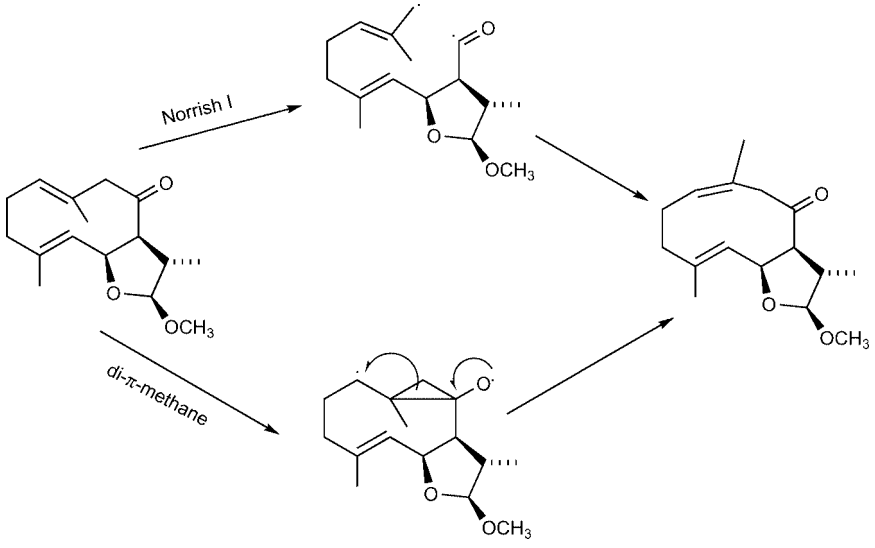


Scheme 2.

  

Table 3. Energies of the four isomers computed at the B3LYP/6-31G(d,p) level and relevant energy differences (1 Hartree = 2625.5 kJ mol$^{-1}$).

| Isomer | Energy [Hartree] | $\Delta E$ [kJ mol$^{-1}$] |
|---|---|---|
| 2 | –849.801025 | $E_3 - E_2 = -15.3$ |
| 3 | –849.806863 | – |
| 4 | –849.801140 | $E_4 - E_2 = -0.3$ |
| 5 | –849.808207 | $E_5 - E_3 = -3.5$ |

tive energy < 8 kJ·mol$^{-1}$[18]) were analysed for both epimers. The values of the four most flexible torsion angles – $\omega_1$ = C1–C2–C3–C4, $\omega_2$ = C2–C3–C4–C14, $\omega_3$ = C15–C10–C9–C8 and $\omega_4$ = C6–C7–C8–O3 – were considered and they are reported in Table 4. It turns out that in the case of the 7β epimer **2** the three low-energy conformers show similar values of the torsion angles $\omega_1$, and $\omega_2$, while $\omega_3$ and $\omega_4$ can assume two different values (bold characters in Table 4). It may therefore be deduced that this epimer can assume three geometrically distinct stable conformations (**conf-2a**, **conf-2b**, **conf-2c**) within the 8 kJ·mol$^{-1}$ threshold, differing only in the positions of the methyl group C15 or of the carbonyl group (Table 4), with a dominant population of the most stable conformer **conf-3a**, very similar to the X-ray structure. On the other hand, in all four stable (again within the 8 kJ·mol$^{-1}$ threshold) conformers of the 7α epimer **3** (**conf-3a**, **conf-3b**, **conf-3c**, **conf-3d**), $\omega_4$ does not change significantly, while the three other torsion angles $\omega_1$, $\omega_2$ and $\omega_3$ all assume two possible values (–48° < $\omega_1$ < +45°, –94° < $\omega_2$ < +93°, –79° < $\omega_3$ < +117°; see bold characters in Table 4). The two methyl groups in **3** can therefore reside

Table 4. Results of the conformational search carried out with the SYBIL forcefield[15] on epimers **2** and **3** in terms of relative stability and relevant torsion angles ($\omega_1$ = C1–C2–C3–C4, $\omega_2$ = C2–C3–C4–C14, $\omega_3$ = C15–C10–C9–C8 and $\omega_4$ = C6–C7–C8–O3). Bold figures represent variations from the X-ray structures (**conf-2a** and **conf-3a**, respectively). Only the conformers with a relative stability within 8 kJ·mol$^{-1}$ are reported.

| | Conformer | $\Delta E$ [kJ mol$^{-1}$] | $\omega$1 [°] | $\omega$2 [°] | $\omega$3 [°] | $\omega$4 [°] |
|---|---|---|---|---|---|---|
| Epimer **2** | **conf-2a** | 0.0 | –50 | –93 | –108 | 88 |
| | **conf-2b** | 4.2 | –26 | –82 | **79** | 71 |
| | **conf-2c** | 6.7 | –50 | –95 | –50 | **–110** |
| Epimer **3** | **conf-3a** | 0.0 | –48 | –94 | –56 | –93.6 |
| | **conf-3b** | 4.2 | **22** | **85** | –79 | –67.3 |
| | **conf-3c** | 6.3 | –25 | –79 | **117** | –66.2 |
| | **conf-3d** | 7.1 | **45** | **93** | **102** | –65.1 |

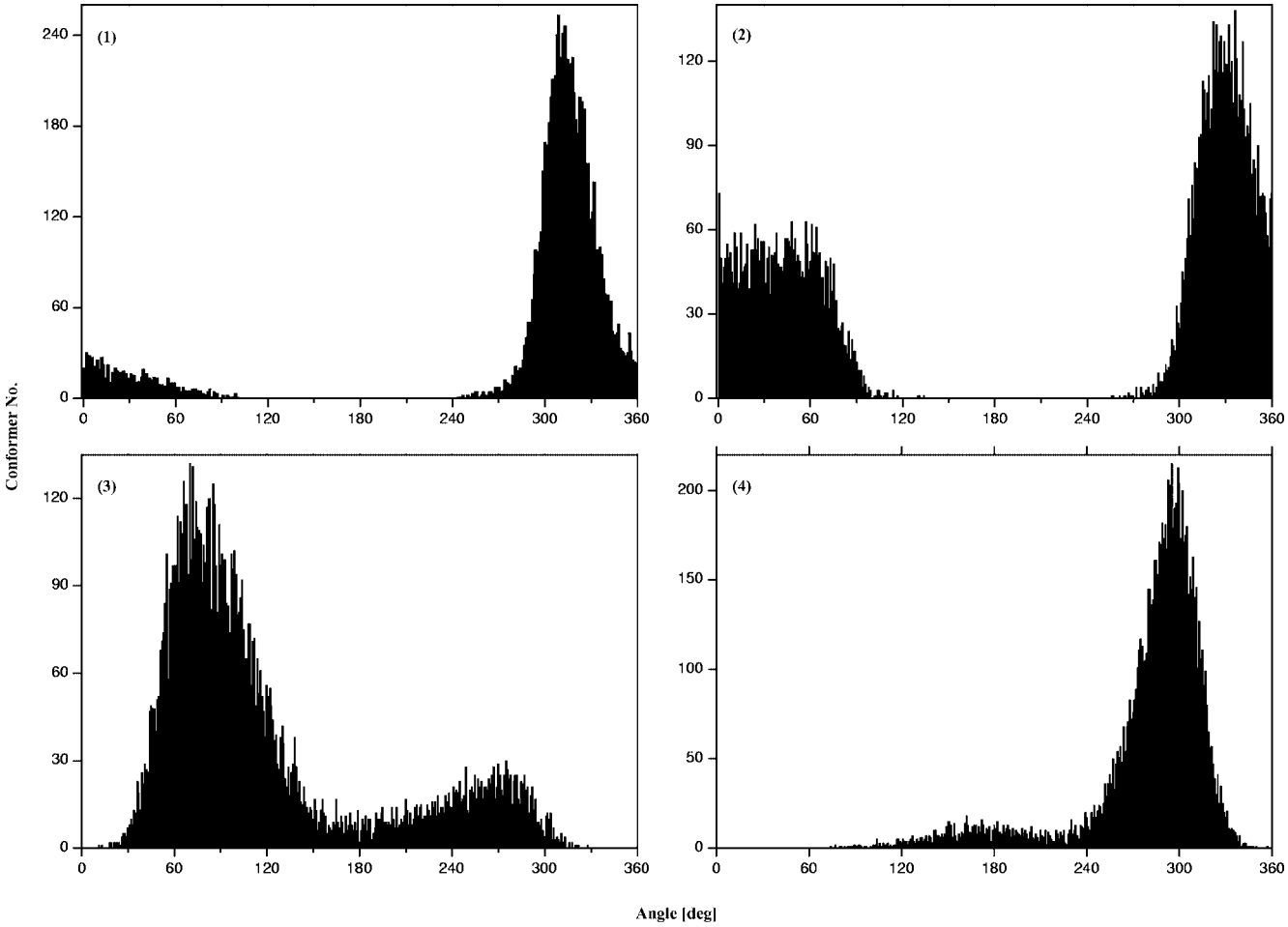


Figure 3. Molecular dynamics simulations: (1) scan of $\omega_1$ (defining the C14 methyl group orientation) for epimer **2**; (2) scan of $\omega_1$ for epimer **3**; (3) scan of $\omega_4$ (defining the carbonyl group orientation) for epimer **2**; (4) scan of $\omega_4$ for epimer **3**.

  

either on the α- or on the β-face, while the carbonyl group is always on the α-face. Also in this case the most stable conformer **conf-3a** (very similar to the X-ray structure) has a prevailing population, but all other conformers together account for one fourth of the total population. These other conformers are significantly different from **conf-3a**, in particular in the positions of the two methyl groups. We may therefore conclude that, in keeping with the NMR results, epimer **3** has a greater conformational variability than **2**.

To provide information on the energy barriers separating the different conformers in Table 4 we carried out two 5 ns MD runs at 800 K on **2** and **3**. These unusually high temperatures (at which **2** and **3** would certainly decompose) were chosen to obtain an exhaustive sampling of their conformational space in a reasonable CPU time (see Exp. Sect. for more details). The results were analysed by representing the distributions of the values of the torsion angles $\omega_1$, $\omega_2$, $\omega_3$ and $\omega_4$ during the simulations (Figure 3). These four torsion angles uniquely define the conformation of the germacrane 10-membered ring.

During the 5 ns simulation on epimer **2**, mobility was observed only around torsion angles $\omega_4$ (Figure 3, plot 3), resulting in a flip-flop motion of the carbonyl group. The remaining larger part of the 10-membered ring proved rather stiff, with the methyl groups C14 and C15 always on the β-face (Figure 3, plot 1 for $\omega_1$), as in the X-ray structure. In the MD simulation on epimer **3**, the carbonyl group does not show a significant mobility (Figure 3, plot 4 for $\omega_4$), probably because it is in the most stable position, far away from the other two oxygen atoms, as indicated by the ab initio calculations. Conversely, the remaining section of the 10-membered ring is flexible and the two methyl groups C14 and C15 can also move to the α-face (Figure 3, plot 2 for $\omega_1$).

Because of the constraints imposed by the ring closure, the motions of all torsion angles in the larger part [C6–C5–C4(C14)–C3–C2–C1–C10(C15)–C(9)] of the 10-membered ring of **3** are mutually dependent. As a result, this moiety is flexible and can assume different conformations. In contrast, as seen earlier, the 10-membered ring of **2** is rather stiff, and only a limited flip-flop motion of the carbonyl group is permitted. These conclusions are in keeping with the results of the conformational search, and can explain the differences in peak widths observed in the NMR spectra of **2** and **3**. It is worth noting that the greater mobility of the 10-membered ring of **3** is also consistent with the large and highly anisotropic atomic displacement parameters in the crystal structure shown in Figure 2.

## Conclusions

Germacrane derivatives are endowed with a remarkable capacity for generating chemical diversity. Thus, provided that an enolizable carbonyl group is present, their well-established cationic chemistry can be complemented by reactions involving anionic and photochemical transformations, setting the stage for the preparation of structurally diverse libraries of unnatural natural products.[19]

X-ray diffraction, NMR spectroscopy and theoretical calculations allowed an exhaustive analysis of the conformational and dynamical features of these medium-sized ring molecules.

## Experimental Section

**General Conditions:** Gravity column chromatography was carried out on Merck silica gel (70–230 mesh); reactions were monitored by TLC on Merck 60 F254 plates, with viewing under UV light at 254 nm, or with 5% $H_2SO_4$ and heating on a hot surface. Melting points were determined with a Büchi SMP 20 apparatus, and are uncorrected. Optical rotations were determined with a Perkin–Elmer 141 polarimeter. IR spectra were obtained with a Perkin–Elmer 257 spectrometer; mass spectrometric data were obtained with a Finnigan LCQ Advantage MS 1.4 spectrometer, fitted with the Xcalibur 1.4 software. $^1$H and $^{13}$C NMR spectra were recorded with a 400 MHz JEOL spectrophotometer; the spectra were recorded in $CDCl_3$ solutions with use of the chloroform signals at δ = 7.26 and 77.1 ppm, respectively, as reference; coupling constants are given in Hz.

**Treatment of 2 with LDA:** A solution of **2** (100 mg, 0.38 mmol) in dry THF (1 mL) was slowly added dropwise to a THF solution of lithium diisopropylamide (0.62 mmol, 1.6:1 molar ratio), and the mixture was stirred in a dry $CO_2$/acetone bath (–78 °C) for 45 min. The reaction was next quenched by the addition of water and allowed to warm to room temp. After extraction with $CH_2Cl_2$, drying ($Na_2SO_4$) and concentration, **2** (89 mg) was recovered as the only reaction product.

**Treatment of 2 with Sodium Methoxide:** Ketone **2** (201 mg, 0.76 mmol) was dissolved in sodium methoxide (2 N, 10 mL), and the mixture was stirred at room temp. for 12 h. The reaction was then quenched with satd. aq. $NH_4Cl$ and worked up by extraction with $CH_2Cl_2$, drying ($Na_2SO_4$) and concentration. Purification by column chromatography (eluent: hexane/ethyl acetate, 3:1), afforded crude **3**, which was recrystallized from acetone at 0 °C to afford crystals (80 mg, 40%).

**7-*epi*-8-Deacyl-8-dehydro-methylhallerin (3):** M.p. 42 °C (acetone). $[\alpha]_D^{20}$ = +58 ($c$ = 0.83, $CH_2Cl_2$). $^1$H NMR ($CDCl_3$): $\delta$ = 5.15 (br. d, $J$ = 11.5 Hz, 1 H, 1-H), 4.96 (br. d, $J$ = 9.8 Hz, 1 H, 5-H), 4.79 (t, $J$ = 9.8 Hz, 1 H, 6-H), 4.62 (s, 1 H, 12-H), 3.53 (br. t, $J$ = 9.8 Hz, 1 H, 7-H), 3.36 (s, 3 H, $OCH_3$), 3.36 (d, $J$ = 9.4 Hz, 1 H, 9a-H), 2.70 (d, $J$ = 9.4 Hz, 1 H, 9b-H), 2.05–1.98 (m, 4 H, 2-H and 3-H), 1.58 (s, 3 H, 14-H), 1.42 (s, 3 H, 15-H), 1.36 (d, $J$ = 7.7, 3 H, 13-H) ppm. $^{13}$C NMR ($CDCl_3$): $\delta$ = 205.1 (s, C-8), 138.5 (s, C-4), 131.2 (d, C-1), 131.0 (d, C-5), 125.8 (s, C-14), 111.7 (d, C-12), 79.8 (d, C-6), 58.7 (q, $OCH_3$), 57.1 (t, C-9), 54.3 (d, C-7), 43.9 (d, C-11), 37.1 (t, C-3), 23.6 (t, C-2), 16.0 (q, C-14), 15.7 (q, C-15), 13.0 (q, C-13) ppm. IR (KBr): $\tilde{\nu}$ = 1695, 1440, 1200, 1080, 1010, 950 cm$^{-1}$. MS (APCI): $m/z$ = 265.4 $[M + H]^+$.

**UV Irradiation of 2:** A degassed solution of **2** (100 mg) in ethanol (10 mL) was irradiated in a Rayonet-type photoreactor with a low-pressure mercury lamp. The course of the reaction was monitored by $^1$H NMR spectroscopy; after 16 h, the isomerization was quantitative. Concentration of the solution afforded **4** in quantitative yield.

**8-Deacyl-8-dehydro-methylisohallerin (4):** M.p. 45 °C. $[\alpha]_D^{20}$ = +98 ($c$ = 0.80, $CH_2Cl_2$). $^1$H NMR ($CDCl_3$): $\delta$ = 5.44 (d, $J$ = 9.2 Hz, 1 H, 5-H), 5.31 (t, $J$ = 7.9 Hz, 1 H, 1-H), 5.08 (dd, $J$ = 9.2, 7.5 Hz 1 H, 6-H), 4.46 (d, $J$ = 4.3 Hz, 1 H, 12-H), 3.46 (s, 3 H, $OCH_3$), 3.45

  

(d, $J$ = 15.1 Hz, 1 H, 9a-H), 2.75 (m, 2 H, 11-H and 7-H), 2.60 (d, $J$ = 15.1 Hz, 1 H, 9b-H), 2.03–1.97 (m, 4 H, 2-H and 3-H), 1.96 (s, 3 H, 14-H), 1.55 (br. s, 3 H, 15-H), 1.13 (d, $J$ = 6.7, 3 H, 13-H) ppm. $^{13}$C NMR ($CDCl_3$): $\delta$ = 207.2 (s, C-8), 138.1 (s, C-10), 132.6 (s, C-4), 124.7 (d, C-1), 124.1 (d, C-5), 112.7 (d, C-12), 76.6 (d, C-6), 62.9 (d, C-7), 56.5 (q, $OCH_3$), 43.7 (t, C-9), 41.0 (d, C-11), 36.7 (t, C-3), 28.5 (t, C-2), 25.7 (q, C-14), 19.5 (q, C-15), 16.5 (q, C-13) ppm. IR (KBr): $\tilde{\nu}$ = 1690, 1460, 1380, 1200, 1140, 1010 cm$^{-1}$. MS (APCI): $m/z$ = 265.3 $[M+H]^+$.

**X-ray Crystal Structure Analyses:** Crystals of **2** and **3** suitable for X-ray analysis were obtained by concentration of acetone solutions. Crystallographic data and details of data collection and refinements have been deposited. CCDC-294952 and -294953 contain the supplementary crystallographic data for this paper. These data can be obtained free of charge from The Cambridge Crystallographic Data Centre via www.ccdc.cam.ac.uk/data_request/cif. Data reduction was carried out by use of the Bruker P3/PC program[20] and Lorentz and polarization corrections were performed. A semi-empirical absorption correction was only applied to the larger crystal of **2**. The structures were solved by direct methods by use of the SIR92 program[21] and refined with the SHELXL-97[22] program. The refinement was by the least-squares, full-matrix method, with anisotropic displacement parameters for all non-hydrogen atoms. The hydrogen atoms were located in calculated positions and treated as riding atoms during the refinement.

**Theoretical Calculations:** The conformational search was performed by molecular mechanics according to the Osawa method[16] as implemented in SPARTAN 5.0,[17] which is capable of handling cyclic molecules, where the torsion degrees of freedom are not independent; the SYBIL force-field[15] was employed. Ab initio DFT calculation based on Becke's[23] three-parameter hybrid functional and the Lee–Yang–Parr[24] gradient-corrected correlation functional (B3LYP) were performed with the Jaguar[25] program. The calculations were carried out on the minimum-energy conformations indicated by the SYBIL conformational search for all four isomers **2**, **3**, **4** and **5**. Accurate estimates of the relative energies were derived by geometry optimization of the four molecules, carried out by ab initio calculations at the B3LYP/6-31G(d,p)[26] level. The graphic analysis was performed with the MOLDRAW program.[27] Finally, the energy barriers between the different conformers were analysed by molecular dynamics (MD) simulations at different temperatures with software from MSI. MD simulations were performed on the isolated molecules **2** and **3**, with use of Discover 3,[28] and graphical display was performed with Insight-II.[29] The equations of motion were integrated with the Verlet leapfrog algorithm[28,30,31] with a time step of 1 fs; the force field used was CFF91,[28] which employs a quartic polynomial for bond stretching and all the cross-terms up to third order, which have been found to be important.[31] In order to observe significant conformational changes in a computationally feasible time, the MD simulations had to be carried out at a sufficiently high temperature to overcome the relatively high energy barriers between possible conformers of the germacrane system. Some MD simulations were therefore first run for 1 ns (after equilibration for 0.01 ns) at different temperatures (300, 400, 500, 600, 700, 800, 900, 1000 K), in order to estimate the temperature needed to explore the conformational spaces of **2** and **3** exhaustively in a reasonable CPU time. These preliminary MD calculations indicated that, during the 800 K MD runs, the conformational changes occur at the ps timescale. Then MD simulations at 800 K (the lowest temperature at which motions cause significant conformational changes) were run for 5 ns (after equilibration for 0.05 ns) on **2** and **3**, in order to obtain an exhaustive description of their conformational motions. Only the results of these 5 ns MD simulations are presented.

## Acknowledgments

Special thanks to Dr. Ivana Fenoglio (University of Torino) for providing us with valuable information on her master thesis work, and to Dr. Gabriele Ricchiardi (University of Torino) for help in the use of computational chemistry software. Financial support from the University of Piemonte Orientale "A. Avogadro" is acknowledged.

[1] J. D. Connolly, R. A. Hill, *Dictionary of Terpenoids*, Chapman & Hall, London, **1991**.
[2] N. Bülow, W. A. König, *Phytochemistry* **2000**, *55*, 141–168, and references therein.
[3] G. Appendino, J. Jakupovic, G. Cravotto, M. Biavatti-Weber, *Tetrahedron* **1997**, *53*, 4681–4692.
[4] G. Appendino, M. G. Valle, P. Gariboldi, *Phytochemistry* **1987**, *26*, 1755–1757.
[5] R. W. Doskotch, C. D. Hufford, F. S. El-Feraly, *J. Org. Chem.* **1972**, *37*, 2740–2744.
[6] H. Yoshioka, T. J. Mabry, A. Higo, *J. Am. Chem. Soc.* **1970**, *92*, 923–927.
[7] R. E. K. Winter, R. F. Lindauer, *Tetrahedron* **1976**, *32*, 955–959.
[8] G. Appendino, P. Gariboldi, *J. Chem. Soc., Perkin Trans. 1* **1983**, 2017–2026.
[9] M. Calleri, G. Chiari, D. Viterbo, *J. Chem. Soc., Perkin Trans. 1* **1983**, 2027–2029.
[10] G. Appendino, G. Chiari, P. Ugliengo, D. Viterbo, *J. Chem. Soc., Perkin Trans. 2* **1987**, 215–218.
[11] G. Appendino, P. Gariboldi, M. G. Valle, *Gazz. Chim. Ital.* **1988**, *118*, 55–59.
[12] In addition to epimerization at C-7, treatment of **2** with NaOMe at room temp. also yields more complex products formed by aldol condensation reactions, G. Appendino, unpublished results.
[13] F. Bohlman, J. Jakupovic, A. Schuster, *Phytochemistry* **1983**, *22*, 1637–1644.
[14] S. Inayama, J. F. Gao, K. Harimaya, L. Litaka, Y. T. Guo, T. Kawarnata, *Chem. Pharm. Bull.* **1985**, *33*, 1323–1326.
[15] M. Clark, R. D. Cramer III, N. Van Opdenbosch, *J. Comput. Chem.* **1989**, *10*, 982–1012.
[16] a) H. Goto, R. Osawa, *J. Am. Chem. Soc.* **1989**, *111*, 8950–8951; b) H. Goto, R. Osawa, *J. Chem. Soc., Perkin Trans. 2* **1993**, 187–198.
[17] Spartan IBM, version 5.0.2X11AIX4.1.4, Wavefunction Inc., Irvine, CA, USA, **1997**.
[18] This threshold value corresponds to a 95% population at 298 K according to the Boltzmann distribution.
[19] G. Appendino, G. C. Tron, T. Jarevang, O. Sterner, *Org. Lett.* **2001**, *3*, 1609–1612.
[20] Bruker, *P3/PC Diffractometer Program*, Version 3.13, Bruker Analytical X-ray Systems, Inc., Madison, Wisconsin, USA, **1989**.
[21] A. Altomare, G. Cascarano, C. Giacovazzo, A. Guagliardi, M. C. Burla, G. Polidori, M. Camalli, *J. Appl. Crystallogr.* **1994**, *27*, 435–436.
[22] G. M. Sheldrick, *SHELXL-97*, University of Göttingen, Germany, **1997** (http://shelx.uni-ac.gwdg.de/SHELX/).
[23] A. D. Becke, *J. Chem. Phys.* **1993**, *98*, 5648–5652.
[24] C. Lee, W. Yang, R. G. Parr, *Phys. Rev. B: Condens. Matter* **1988**, *37*, 785–789.
[25] *Jaguar 5.5*, Schrödinger Inc., Portland, OR, USA, **2003**.
[26] W. J. Hehre, L. Radom, P. v. R Schleyer, J. A. Pople, *Ab initio molecular orbital theory*, 1st ed., John Wiley & Sons, New York, **1986**, chapter 4.

  

[27] P. Ugliengo, D. Viterbo, G. Chiari, *Z. Kristallogr.* **1993**, *207*, 9–23 (http://www.moldraw.unito.it).
[28] *Discover 2.9.8/96.0/4.0.0 User guide*, MSI, 9685 Scranton Road, San Diego, CA 92121-3752, USA, **1996**.
[29] *Insight-II User Guide*, version 4.0.0, MSI, 9685 Scranton Road, San Diego, CA 92121-3752, USA, **1996**.
[30] A. R. Leach, *Molecular Modeling Principles and Applications*, Addison Wesley Longman, Harlow, Essex, UK, **1996**, pp. 313–370.
[31] J. R. Maple, T. S. Thacher, U. Dinur, A. T. Hagler, *Chemical Design Automation News* **1990**, *5*, 5–10.

Received: February 7, 2006
Published Online: May 12, 2006

  